


Article

On Capabilities of Tracking Marine Surface Currents Using Artificial Film Slicks

Ivan A. Kapustin ^{1,2,*} , Olga V. Shomina ¹, Alexey V. Ermoshkin ¹, Nikolay A. Bogatov ¹, Alexander V. Kupaev ¹, Alexander A. Molkov ^{1,2} and Stanislav A. Ermakov ^{1,2}

¹ Institute of Applied Physics of the Russian Academy of Sciences, 46 Uljanova St., Nizhny Novgorod 603950, Russia; seamka@yandex.ru (O.V.S.); al-ermoshkin@yandex.ru (A.V.E.); nbogatov@ipfran.ru (N.A.B.); sant3@mail.ru (A.V.K.); wave3d@mail.ru (A.A.M.); stas.ermakov8@gmail.com (S.A.E.)

² Volga State University of Water Transport, 5 Nesterova st., Nizhny Novgorod 603005, Russia

* Correspondence: kapustin-i@yandex.ru; Tel.: +7-831-416-48-59

Received: 13 March 2019; Accepted: 4 April 2019; Published: 8 April 2019



Abstract: It is known that films on the sea surface can appear due to ship pollution, river and collector drains, as well as natural biological processes. Marine film slicks can indicate various geophysical processes in the upper layer of the ocean and in the atmosphere. In particular, slick signatures in SAR-imagery of the sea surface at low and moderate wind speeds are often associated with marine currents. Apart from the current itself, other factors such as wind and the physical characteristics of films can significantly influence the dynamics of slick structures. In this paper, a prospective approach aimed at measuring surface currents is developed. The approach is based on the investigation of the geometry of artificial banded slicks formed under the action of marine currents and on the retrieval of the current characteristics from this geometry. The developed approach is applied to quasi stationary slick bands under conditions when the influence of the film spreading effects can be neglected. For the stationary part of the slick band where transition processes of the band formation, e.g., methods of application of surfactants on water, film spreading processes, possible wind transformation etc., become negligible, some empirical relations between the band geometrical characteristics and the characteristics of the surface currents are obtained. The advantage of the approach is a possibility of getting information concerning the spatial structure of marine currents along the entire slick band. The suggested approach can be efficient for remote sensing data verification.

Keywords: film slick; slick band; sea surface; surface current structure

1. Introduction

It is well known that films on the sea surface can indicate the presence of various geophysical processes in the upper ocean layer and in the atmosphere, for example, internal waves, fronts, convective atmospheric cells, etc. [1–5]. In particular, banded slick structures that appear in SAR images of the sea surface at low and moderate wind speeds are often associated with marine currents. Usually it is ‘a priori’ considered that slick bands mark fine structure of currents/eddies, manifested as “filaments” in sea surface imagery [6,7].

The sources of slick features in the SAR imagery can be illegal ballast water discharges, river and collector drains, biogenic surfactants, ship wakes, etc. Consequently, slick structures can indicate the dynamics of near surface processes, since surfactants can accumulate, for example, in the areas of current convergence zones [8–11] or can appear in shear stream currents [12].

It should be noted that in addition to the sea currents, other factors can significantly influence the dynamics of slicks and their geometry. A number of papers indicate the need to take into account the influence of the wind on the propagation of slicks. In particular, it is declared in [13–17] that the

influence of wind-wave drift is significant and should be taken into account when interpreting results of observations of slicks, although the drift under real sea conditions seems to be quite difficult to determine. In addition, slick dynamics strongly depend on the viscoelastic characteristics of surfactants, whose chemical composition and concentration are in general unknown.

The capabilities of remote sensing instruments for measuring marine currents are widely discussed in the literature. The problem of radar measurements of marine currents with radar is, in general, complicated and not completely resolved at present. HF radars ([18], and references there in) are successfully used for current monitoring in coastal zones, and the retrieved current velocity relates to the upper water layer of which the thickness ranges from tens of cms up to around one meter. This can only be roughly relevant to the problem of oil pollution forecasting, since oil spill movement is determined by current velocities in the upper microlayer with depths of the order of 1 mm or less. A disadvantage of HF radar systems is the need for a large antenna system and the impossibility to deploy the systems at any site of the coast. More relevant to the problem of oil spill transport can be microwave measurements with Doppler scatterometers or SAR [19–22], which can give information about velocities in the upper thin water layer with thickness of about 1 cm or less. However, the difficulty arising here is that the intrinsic scatterer's velocities, either the velocities of free and/or bound Bragg gravity-capillary wave, typically cm-scale waves, or scatterers associated with micro breaking of longer gravity waves are poorly known [21–23]. Accordingly, this insufficient knowledge results in some uncertainties in current velocity estimates. However, one can use SAR to retrieve marine currents from the imagery of slicks of the sea surface, in particular, when analyzing the geometry of artificial slick bands. The geometry can also give valuable information in the context of the problem of oil film transport since there is lack of methods of the current velocity measurements in the surface microlayer. Meanwhile, particularities of spreading and drift of film slicks, which are closely related to the structure of near-surface current and environmental conditions in the area of interest, can be considered as a source of information for remote sensing systems [24–29]. A possible way to use slicks for tracking marine surface currents and, moreover, to retrieve their quantitative characteristics, is to create slicks with known properties and geometries.

In this paper, a promising approach for estimating marine currents is developed, based on the formation of long slick bands with given initial characteristics and on recording the band geometry. The results of the first experiments with artificial slick bands are presented, and the prospective capabilities of the developed approach are discussed in the application to the problem of remote sensing of surface currents. The results may be of particular importance when interpreting high-resolution satellite data in terms of the analysis of the structure of marine currents in a given area.

2. Materials and Methods

2.1. Experimental Technique

The technique is based on the continuous deposition of surfactants on the sea surface when releasing surfactants from a tank over an extended period of time. At a certain distance from the tank a slick band is formed, which is moved by a surface current and, accordingly, marks its structure. Measurements using the described method can be carried out from fixed sea platforms or from anchored vessels. Wind-wave conditions impose certain restrictions on the possibility of conducting experiments with artificial slick bands. The method cannot be used in completely calm or stormy conditions, since the slick either does not have contrast towards surrounding water or will be quickly mixed down due to wave breaking. However, the interval of appropriate wind speeds is quite wide and ranges from 2 to 10 m/s. The general algorithm for implementing the suggested method is as follows:

1. Creation of an artificial slick band by continuous outflow of surfactants from a tank installed at a given point in the water area.

2. Simultaneous continuous or periodic registration of meteorological parameters and the current velocity near the tank. Periodic registration of characteristics of the area covered by surfactant film with remote sensing instruments particularly satellite-based ones. Any accompanying information may be useful, such as the characteristics of surface waves, thermohaline structure, optical properties of seawater. The accompanying information can help in interpreting the experimental data, for example, to identify an artificial slick band towards the background of natural slicks.

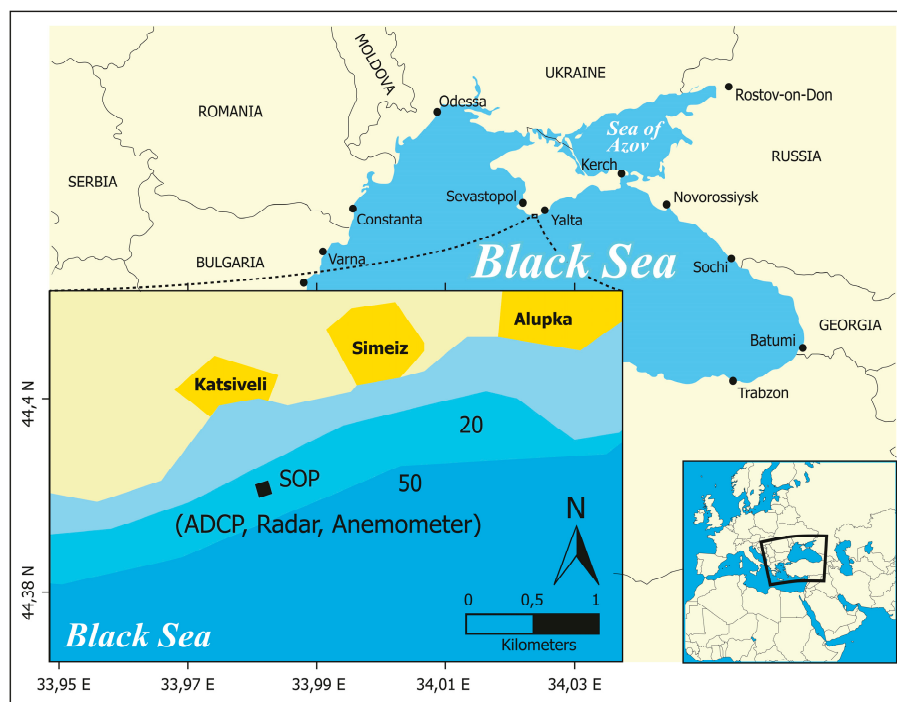
3. Retrieval of subsurface currents characteristics in the observed water area according to the registered structure of an artificial slick band.

The implementation of the third point, generally speaking, implies knowledge of the empirical relationships between the characteristics of slick bands, currents and near-surface wind.

Unlike observations of dynamics of natural slick bands, the use of artificial bands provides several advantages. In particular, viscoelastic characteristics of used surfactant films can be known for the artificial slick bands and, in addition, experiments with artificial slicks imply the use of surfactants that do not cause any damage to the marine environment. These can be vegetable oils (VO) or organic fatty acids, for example, pure oleic acid (OLE), often used in experiments with artificial slicks [23–29].

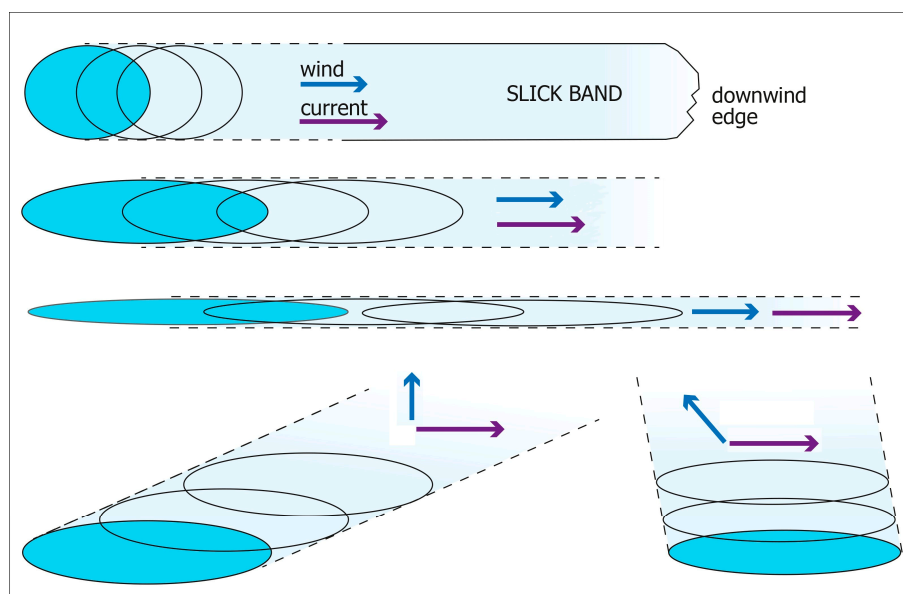
Experimental testing of the proposed methodology was carried out on the Stationary Oceanographic Platform (SOP) of the Black Sea Hydrophysical Polygon, the Russian Academy of Sciences. The location of the SOP on the map is shown in Figure 1a.

An artificial slick band was created by continuous outflow (dripping) of OLE and VO from a plastic tank with a 1.5 mm diameter hole in the bottom installed on the middle deck of the SOP at a height of 4.2 m. The process of slick band formation at different current directions and wind velocities is shown schematically in Figure 1b.



(a)

Figure 1. Cont.



(b)

Figure 1. (a) A map of the study area. (b) Schematic representation of an artificial slick band formation at various speeds and directions of the near-surface wind and current.

Surfactant drops from a plastic tank fall on the sea surface and spread out, forming a “single” slick—a certain elementary part of the band (shaded area in Figure 1b). It is well known that slicks in the process of spreading are stretched along the wind direction and their center of mass moves in the direction of the resulting surface velocity; the single slick spreads out and drifts away, and the next one is formed on its place. This results in the formation of a band consisting of individually spreading film slicks.

Depending on the direction of both wind and current, as well as a relation between their speeds, the formation of bands with different scales, geometry, in particular, the direction of propagation is possible. If the marine current or wind changes during the band movement, this change affects the band geometry. For the case when the wind field is uniform on the scale of the band the distortions of the latter may allow one to retrieve the current structure.

The duration of the experiment was more than 8 h (18:06–02:26), during this time about 1.5 L of OLE and 3 L of VO were consumed in sequence. An average consumption of surfactant was 8–10 mL per minute.

2.2. Apparatus and Data Processing

The speed and direction of the near-surface wind were measured using a WindSonic ultrasonic anemometer (Gill InstrumentsTM) installed at a height of 20 m, followed by a recalculation to a standard height of 10 m. The frequency of wind measurements was 1 Hz. The speed and direction of the marine current at depths from 1 m to 25 m with a step of 0.5 m were obtained according to the data of the acoustic Doppler current profiler (ADCP WorkHorse Monitor 1200 kHz, RDITM), which was hung out on the cables from the middle deck. The ADCP was oriented vertically downward and was sunk to a depth of 0.3 m, the frequency of the probe pulses (pings) was about 1 Hz. During the subsequent processing, the wind and current measurements were averaged over 2 min in order to be combined with radar images. Serial radar images of the water surface comprising the artificial slick band were recorded using an MRS-1000 digital coherent radar instrument (MicranTM) mounted onto the roof of the SOP (Figure 2) at a height of 18 m above sea level.

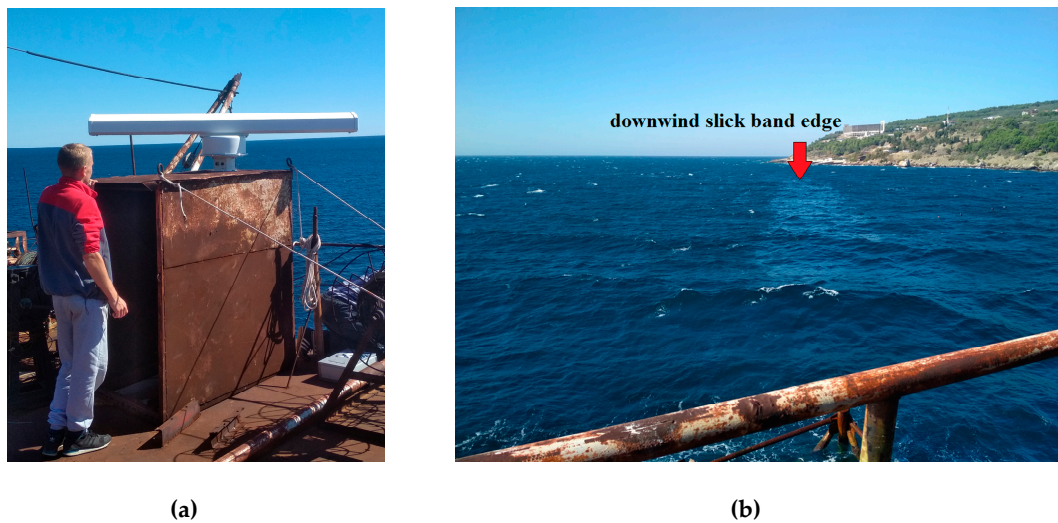


Figure 2. (a) The MRS-1000 radar installed on the SOP. (b) A photograph of an artificial slick band on the sea surface.

The radar operates in a chirp waveform mode of continuous radiation at a frequency of 9.4 GHz (X-band) with a modulation band of 191 MHz at the horizontal polarization of radiation and reception. The rotation period of the radar station antenna can be varied from 2.5 s to 18 s; during the experiment, a slow rotation speed of 4 rotations per minute was used. Non-coherent averaging over 2 min (8 turns of the antenna) makes it possible to eliminate the fluctuations of the reflected radar signal associated with wind waves, as well as to smooth the speckle noise.

A typical radar image containing an artificial slick band is shown in Figure 3. The following features can be seen in the Figure 3: the elongated area (1) of low radar backscatter is the slick band, the bright marks (2) which are anchored oyster farm buoys, the coastline (3), the area of the re-reflected radar signals (4) related to the closely located metal structures, the dead zone of the radar station (5). The radar has a high range resolution of 0.79 m, so that the fine spatial structure of the slick band can be registered (Figure 4a). We prepared one video to explain slick band propagation, please refer to supplementary materials.

Before discussing the results of the experiment, we should determine a set of informative parameters characterizing the artificial slick band. Each fraction of the slick band can be characterized by the direction of propagation (azimuth) and the width. These values are determined using a threshold method of processing of radar images, the dependence of the reflected signal intensity on distance have been preliminary eliminated. The processing is carried out in the polar coordinate system. The angular boundaries of the slick band $D_s^1(r, t)$ and $D_s^2(r, t)$ have been automatically determined while the propagation direction of the band has been defined as

$$D_s(r, t) = \frac{D_s^1(r, t) + D_s^2(r, t)}{2}, \quad (1)$$

and the width W as

$$W(r, t) = 2 \cdot r \cdot \text{TAN} \left(\frac{D_s^2(r, t) - D_s^1(r, t)}{2} \right) \quad (2)$$

where r is the distance from the SOP, t is the time of observation. The definition of the direction and width of the band is illustrated graphically in Figure 4b.

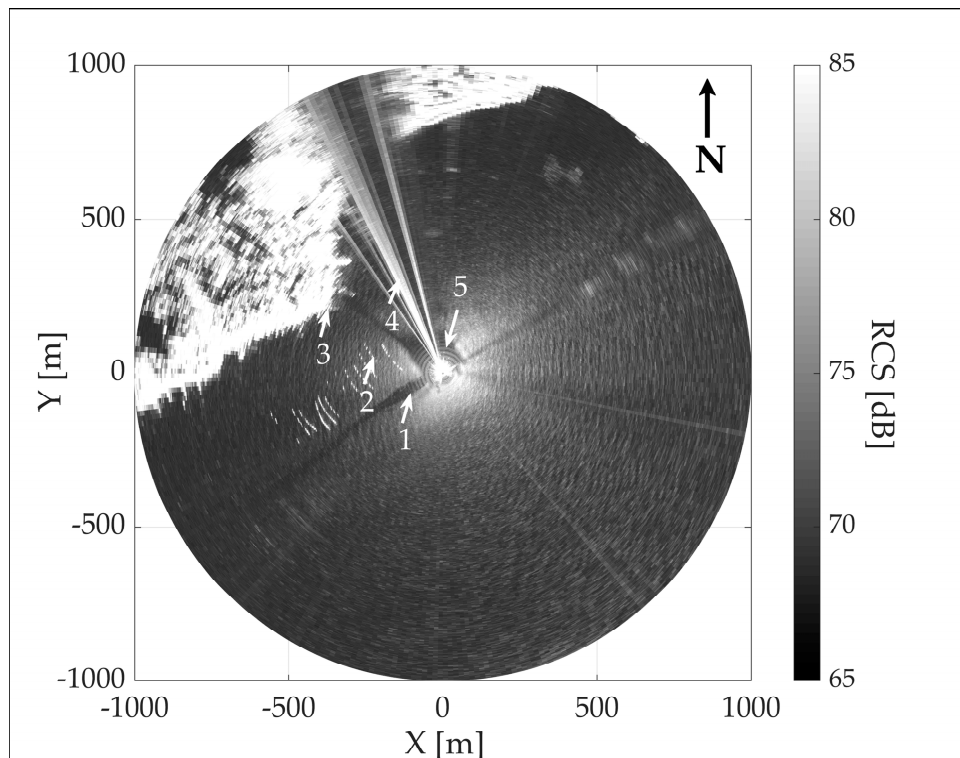


Figure 3. MRS-1000 radar snapshot with an artificial slick band: slick band (1); the anchored oyster farm buoys (2); the coastline (3); the area of the re-reflection (4) the dead zone of the radar (5).

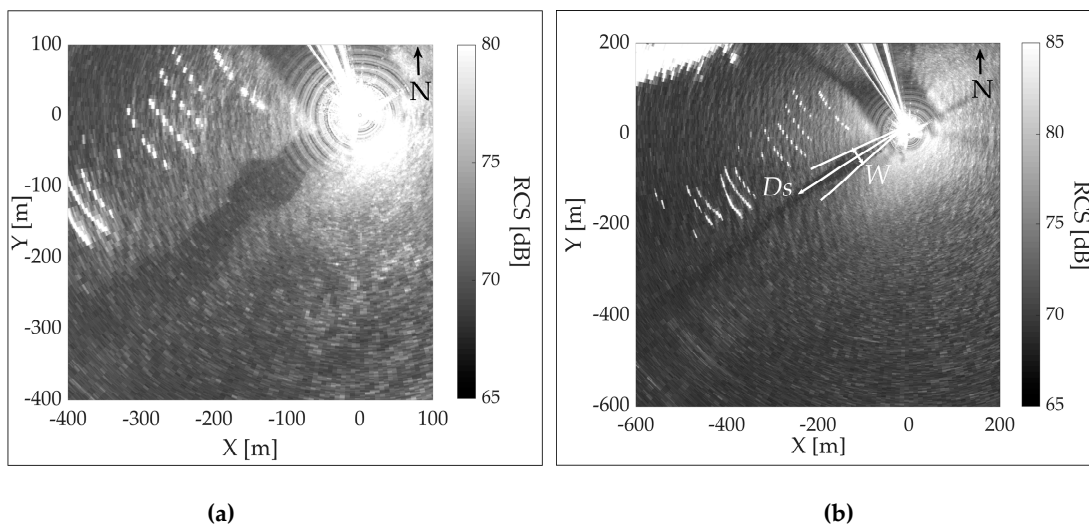
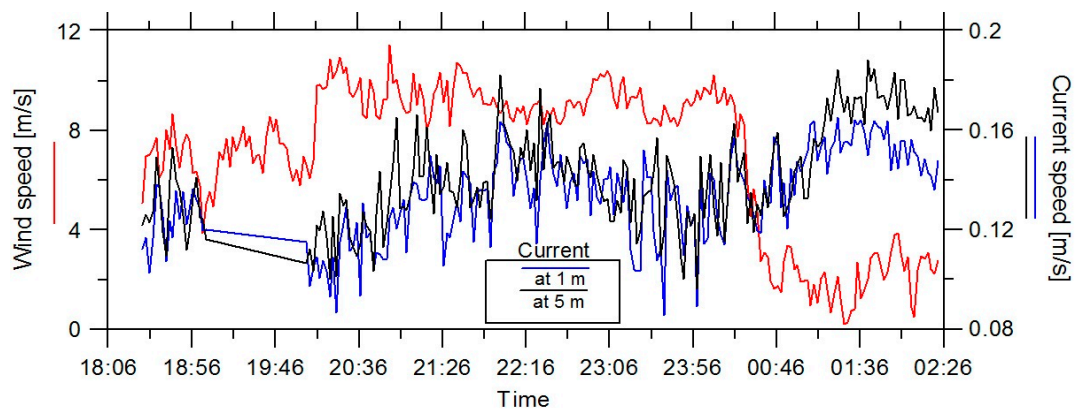


Figure 4. (a) Fine spatial structure of a slick band. (b) Determination of the direction D_s of the slick band and its width W .

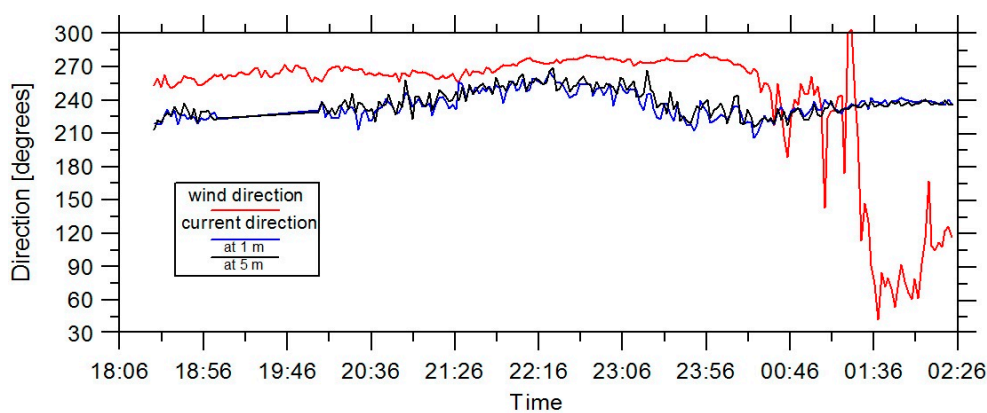
3. Results and Discussion

3.1. Environmental Conditions

Figure 5 shows time series of speed and direction of wind and current during the experiment, all data are presented with an averaging time of 2 min.



(a)



(b)

Figure 5. The measurements of: (a) speeds and (b) directions of wind and current during the experiment. The red curve is wind, black and blue show the current at depths of 1 and 5 m respectively. The direction is measured from the north direction (0 degrees).

Figure 5 shows that the wind speed has been varying during the experiment within the range of 2–10 m/s, the wind most of the time had an eastward direction (about 90 degrees). The wind direction has been turned 180 degrees for convenience of the collation with the current. During the final stage of the experiment, the average wind speed dropped to about 2 m/s and the direction changed by almost 180 degrees. The speed of the near-surface current at the depth of 1 m ranged from 8 to 18 cm/s and the direction varied between 215–255 degrees. The mean difference of current velocities at depths of 1 and 5 m was about 0.5–1 cm/s, the difference between current directions was insignificant (on average of 2 degrees with a standard deviation of 6 degree). There was no data on currents recorded from 19:00 to 20:00.

3.2. Slick Band Formation

The band was reliably recorded in the radar snapshots in less than 3 min after the start of the spill, when the length of the band was about 70 m. Let us consider the process of a banded slick formation and the movement of its downwind edge. Successive radar snapshots showing the formation of the band structure at different times after the beginning of spilling are presented in Figure 6. A slight blurring of the edge of the band on the presented radar snapshots is associated with averaging of the images.

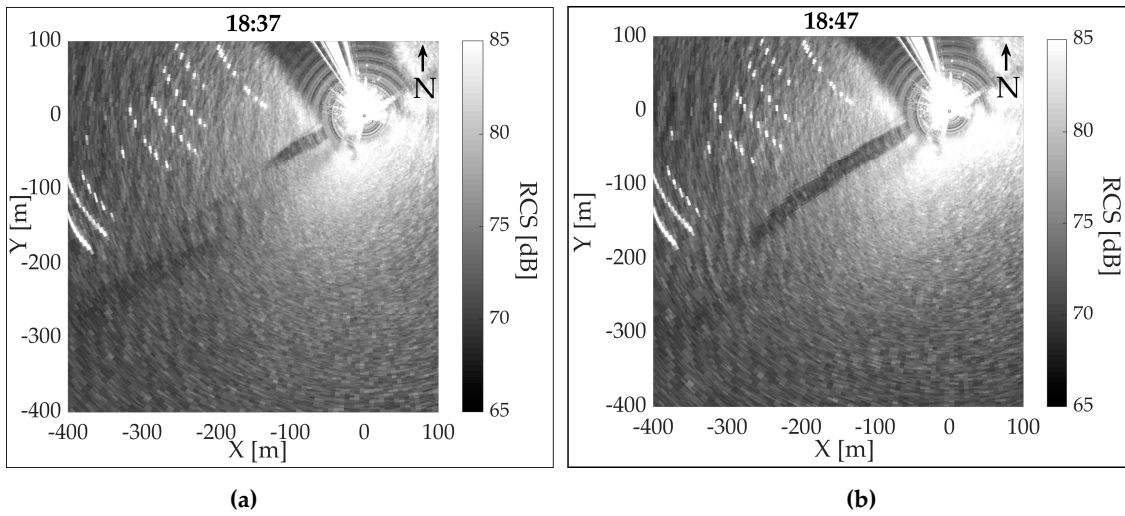


Figure 6. The formation of the band on the radar snapshots at different times: (a) 18:37, (b) 18:47.

The process of formation of the slick band with a visible length of more than 400 m lasted a little longer than 20 min. The band was recorded visually and by the radar. The trajectory of the downwind slick band edge was retrieved from sequential radar snapshots. The obtained trajectory is presented in Figure 7.

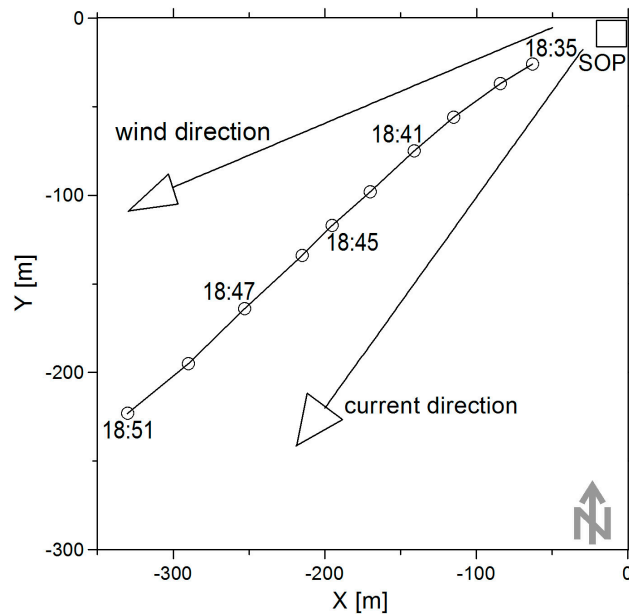


Figure 7. The trajectory of the downwind slick band edge. The rectangle schematically indicates the SOP, the circles indicate the downwind edge band structure position, the arrows show the average wind and current directions during the band formation. Distances along the axes North (Y) and East (X) of the SOP are given in meters.

It can be concluded from Figure 7 that the band edge has been moving in the sector between the directions of wind and current. One should note that the movement of the band edge was not uniform and rectilinear. The direction of the band edge movement, as well as the directions of the current and wind, are presented in Figure 8a; the corresponding velocities are shown in Figure 8b.

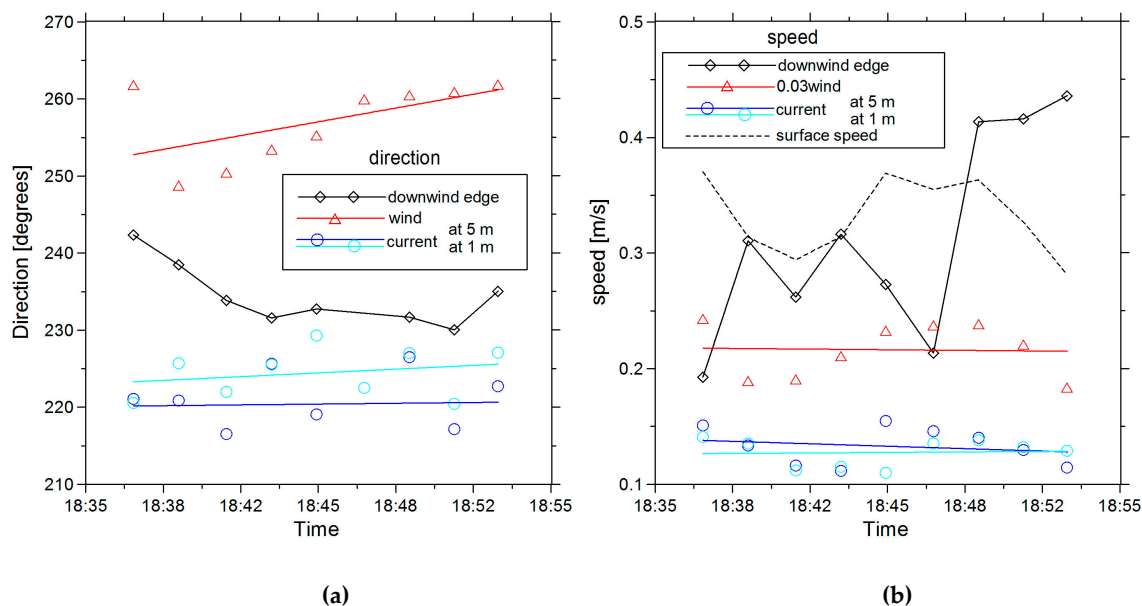


Figure 8. (a) Direction and (b) speed of the downwind band edge movement (black diamonds), wind (red) and current (blue—1 m, cyan—5 m depth). The dashed curve is the total surface velocity calculated as the sum of the current velocity and wind drift vectors. The wind drift speed is taken as 3% of wind speed and is denoted by the red symbols (triangles).

Figure 8a shows how the band direction has been changing as the downwind band edge has been moving away from the SOP. The band direction has been getting closer to the current direction, thus illustrating the important role of wind at the initial stage of the slick band formation. The band edge speed (see, Figure 8b) is, on average, of 0.3 m/s, which corresponds to the current velocity summed with wind-wave drift that is to the speed of film advection as if the surfactants are passive substances. In other words, the fact that the velocity of the downwind edge is close to the velocity of a thin surface layer shows that the film spreading process does not contribute to the velocity of the downwind edge, at least at large enough band lengths.

According to our estimates, direct action of wind is accumulated in the upper layer with thickness of the order of 1 m and less [15]. Hereafter, when talking about “marine currents”, we mean the movement of a water layer of the order of 1 m depth and deeper. By the “surface velocity” we denote the velocity of a thin top layer of about mm-to-cm thickness, which is affected by the combined action due to both wind drift and current and affects the slick movement.

One can now estimate at what distances the film spreading of the downwind edge of the band may weakly contribute to the total band edge velocity. When considering spreading at the downwind band edge one can neglect the action of wind waves and estimate the spreading speed from the balance between the surface tension and viscous stresses [30] as follows:

$$\Delta\sigma \propto \alpha \cdot \rho \cdot u_s^2 \sqrt{\nu t} \quad (3)$$

where $\Delta\sigma$ is the film pressure, i.e., a difference between surface tension coefficients in the background water surface and inside a film slick. The film pressure for saturated OLE films is about 40 mN/m, see, [31], ν is the kinematic water viscosity, t is the spreading time, ρ is the water density, u_s is the spreading speed, α is an empirical coefficient, the latter was estimated from our previous field studies of the spreading regimes of OLE slicks as about 3 [17]. Equation (3) is equivalent to the well-known Fay’s spreading law and predicts the spreading speed u_s which decreases with time as $t^{-1/4}$. For the case of the film advection due to the surface speed u_c the spreading time is obviously $t = L/u_c$, where L is the band length. Then one can easily obtain that the spreading speed significantly decreases at sufficiently large distances. For example, u_s drops to about $0.1 \cdot u_c$ that is in our experiment about

2.5 cm/s at distances $L \sim 10^2$ m, so that film spreading effects at distances about or larger than 10^2 m are small compared to the film advection due to the current. Therefore, the distance for analysis of the slick edge is chosen below as 150 m.

3.3. Slick Band Direction (Azimuth)

Let us consider now the characteristics of the slick band. For the analysis of azimuth angle of the band, the time period of 18:30–00:20 was chosen, when a relatively stable wind direction was observed (Figure 5). The wind contribution to the characteristics of slick band propagation was estimated by minimizing the standard deviation of the band azimuth at the distance of 150 m from the direction of the vector $u_c + nW$, where u_c is the current velocity, W is the wind velocity, and n is an empirical coefficient. The smallest deviation was observed when the current was at 1 m depth and $n \sim 2\text{--}3\%$.

Additionally, we analyzed correlation between the directions of the band and the total surface current. The correlation was found to achieve a maximum value when the wind-wave drift was assumed to be 3% of the wind speed. It can be concluded that the propagation of the band can be described by the sum of current in the upper layer and of 3% of wind speed (Figure 9).

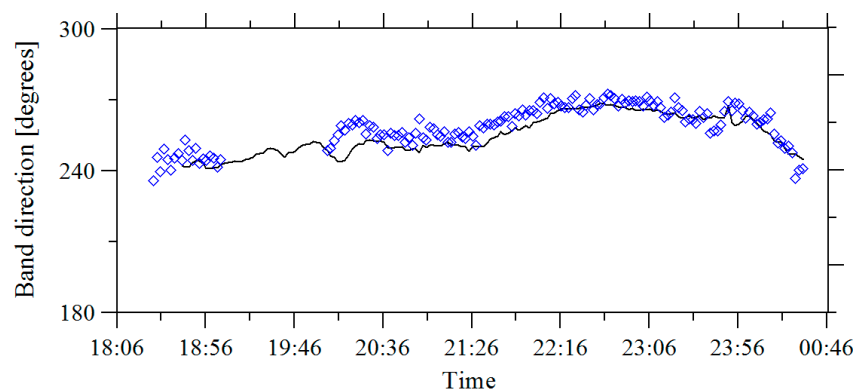


Figure 9. The band propagation direction D_s at a distance of 150 m from the SOP (black line) and the direction of the vector of the sum of the current speed in the upper layer and 3% of the wind speed (blue diamonds).

Figure 10 presents the positions of the slick band at different times in order to compare with band edge positions. It also indicates the directions of wind and current. Figure 10a describes the “reaction speed” of the band structure to a change of the wind direction. The band have been formed at 18:51, and the averaged image is obtained at 18:55. It is seen that at short distances from the SOP, the band does not react to the change of the wind direction, while at distances larger than 130 m, the change of the band direction becomes noticeable. This indicates again that the remote part of the band is the most informative. Figure 10b,c show how the direction of the band have changed after amplification and reduction of wind speed, respectively. Figure 10d indicates the effect of the band leaving the wind-current sector due to an abrupt, 180 degrees change in the wind direction. After the sharp reduction at 0:46 and the changed direction of the wind at 01:36, the band structure reformed along the current. At low wind speeds, the width of the band significantly increased and the morphology of the band became complicated; as a result, the determination of the band direction may be very difficult. Since the surfactants used in the experiment have similar physical characteristics (surface tension coefficients and elasticity), no significant difference between their dynamics is observed.

It should be noted that the downwind band edge movement is described at much greater distances from the SOP than the formed band (Figure 10). A small array of radar snapshots containing the band downwind edge was processed “manually”, and for the main data array of radar snapshots, special software was developed that allowed us to process a large number of snapshots automatically. The sensitivity of “manual” processing, due to objective reasons, was higher.

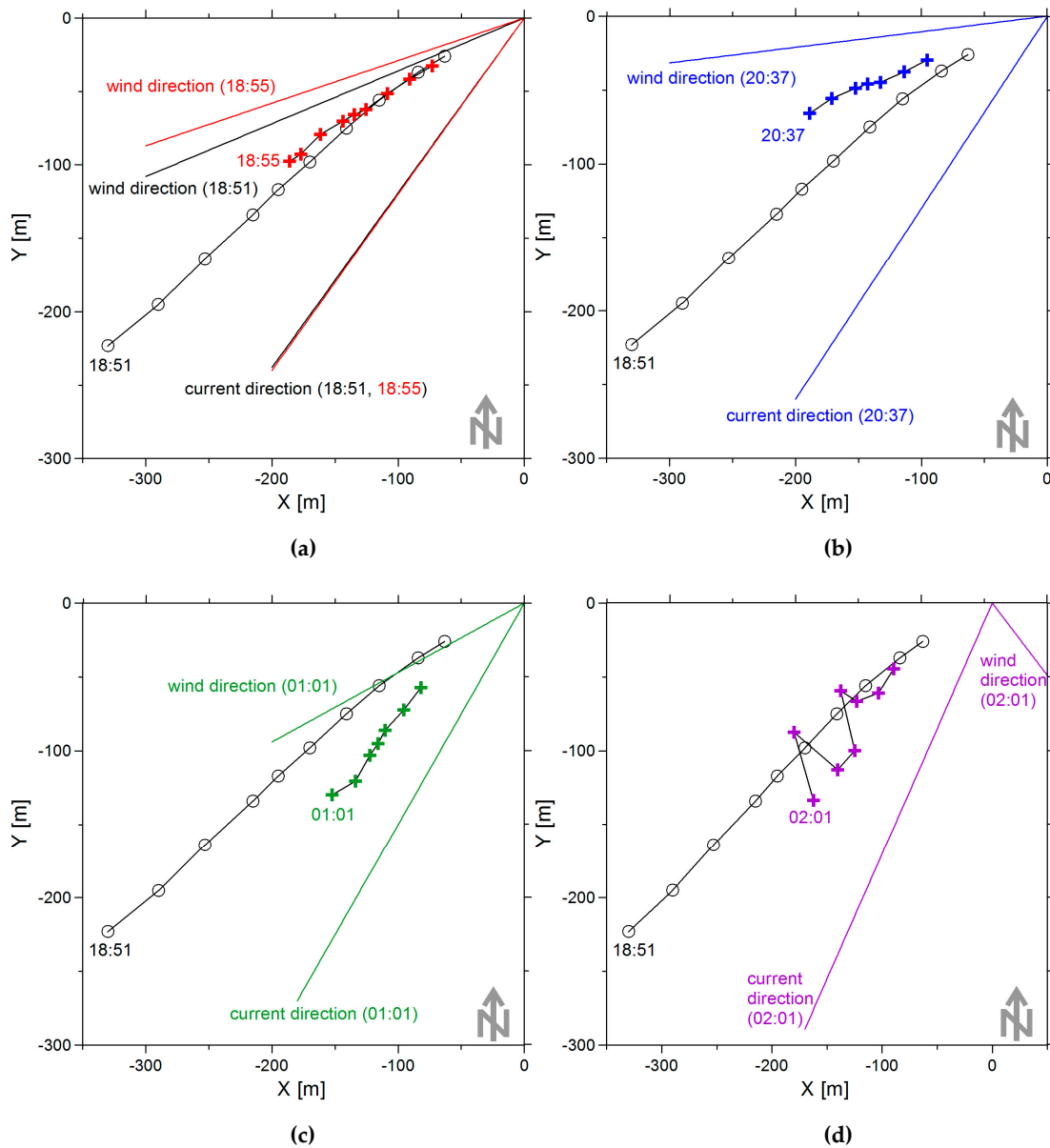


Figure 10. The positions of the slick band at different times relative to the originally formed: (a) 18:55, (b) 20:37, (c) 01:01, (d) 02:01. Straight lines denote the sector formed by the directions of wind and current at the time of the image of the slick band.

3.4. Slick Band Width

Let us now consider the behavior of the slick band width as a function of surface speed at fixed distances from the SOP (100, 150, 200 m). Figure 11 shows typical radar snapshots for relatively high (a) and low (b) surface velocities. An average current velocity during the experiment was about 12–14 cm/s; the contribution of wind speed to the surface velocity could be estimated as 18–30 cm/s at the beginning of the experiment and 7–5 cm/s at the end.

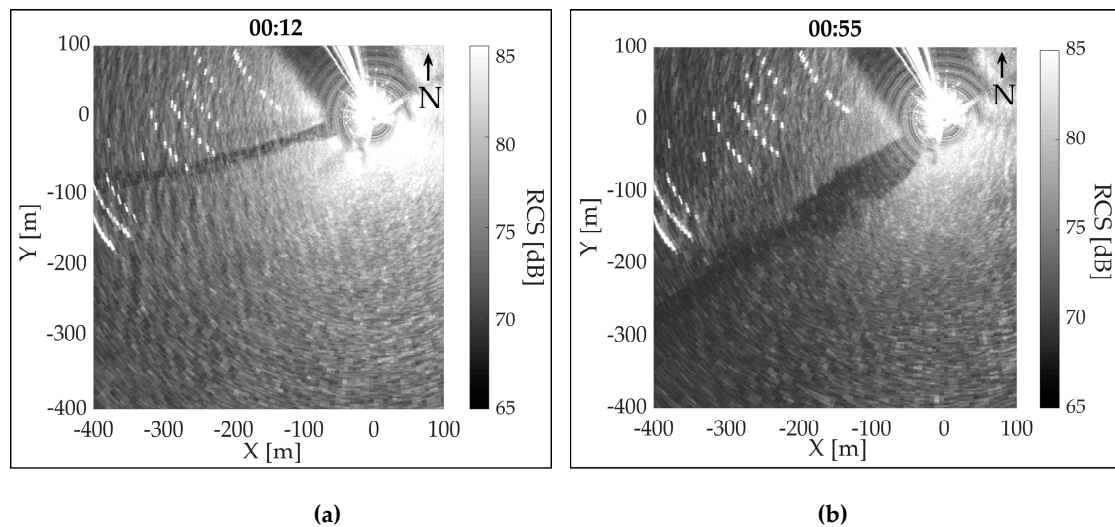


Figure 11. Examples of radar snapshots of slick band at different surface velocities: (a) 0.42 m/s, (b) 0.23 m/s.

The experimental values of the slick band width plotted against the measured surface speed and the best fit approximation of the data (solid black curve) are shown in Figure 12a. The best fit curve is rather close to an inverse proportional dependence $W = 8.2 \cdot u_c^{-1}$ (RMSE = 17 m, number of points $N = 534$), which means that surfactants have been evenly distributed in the slick band, i.e., the surfactant concentration in the band remains nearly the same at different distances from the source. This conclusion can be explained as follows. The surfactant concentration in the band can be estimated using the mass conservation law in the form

$$C = \frac{\rho f}{u_c W} \quad (4)$$

where u_c is the surface speed, ρ is the surfactant density, W is the band width, f is the consumption of surfactant flow, i.e., the volume of released surfactants per unit time. Since the values ρ and f are known constants, one can expect that, when taking into account the dependence $W(u_c)$ in Figure 12a, C is roughly constant, too. The surfactant concentration values C estimated from data in Figure 12a are shown in Figure 12b, and the best fit of the C -values (the horizontal black line in Figure 12b) indicates that the conclusion about constant surfactant concentration in the slick band is justified (MEAN(C) = 16.1 mg/m², RMSE = 6 mg/m², number of points $N = 534$). The mean concentration was found as an arithmetic mean of N values. The RMSE was found using the least squares method.

The obtained dependences indicate that at distances greater than 100 m from the SOP, the band can be characterized by a constant width, and the band spreading effects no longer manifest, since the scatter plots are uniform and do not separate depending on the distance from the SOP. The large scatter of points at lower surface velocities can be explained by the difficulties associated with slick band contouring under these conditions (Figure 11b). The calculated surface concentration of surfactants remains approximately constant over a wide range of surface speeds. This leads to the constancy of $u_c W$ along the slick band, and this fact makes it possible to retrieve the fine structure of the surface speed along the slick band.

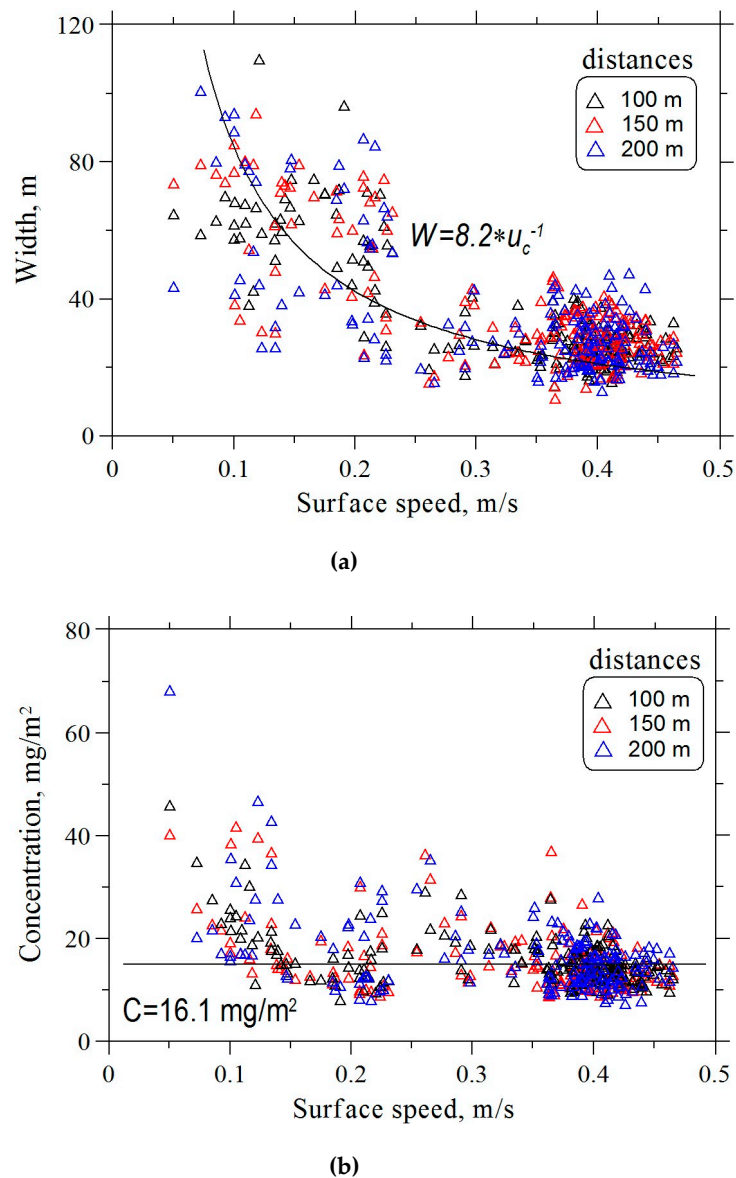


Figure 12. (a) Band width W and (b) surfactant concentration C as functions of surface speed u_c at different distances from the SOP. Black curve is the best fit approximation of experimental data.

Note that the conclusion about the nearly constant (or slowly changing) band width at large enough distances is consistent with the results of previous experiments on film spreading and with a respective model [17]. Now we give a physical explanation why the band of roughly constant width can form.

Spreading of films in the presence of wind waves is controlled by surface tension, viscous stresses and stresses induced by surface wind waves. The surface tension forces act at the slick boundary resulting to slick extension since the surface tension within slick is smaller than for surrounding clean water. So, the surface tension leads to film spreading. The stresses induced by wind waves are proportional to the squared wind wave amplitude (or, more correctly, to the wind wave spectrum) and act along the wave propagation direction. The wave stresses in the slick just after the waves have entered the slick are larger than for clean water, because of the enhanced wave damping in the film covered area. Wind waves obliquely entering into slick through its boundaries parallel to the wind act on film via the cross-wind projection of the wave induced stresses τ_{\perp} oppositely to the surface tension forces. Therefore, wave stresses can partly compensate or even exceed the surface tension forces, thus reducing the effect of film spreading or even leading to film compression. It follows

from theory [17] that a slick with a constant width can be realized as a result of the equilibrium between surface tension and induced wave stresses; the friction forces at this equilibrium are zero. The equilibrium width can be roughly estimated as $W \propto \Delta\sigma/\tau_{\perp}$. Using the values of induced stresses calculated in [17] for an empirical wind wave spectrum [32] at moderate winds, we can estimate a stable band width of about 10 m. This estimate of the stable width is roughly consistent with our observations.

3.5. Retrieval of Marine Currents

In fact, many slick bands occurring on sea surface and propagating over long distances are most often associated with the long-term and relatively permanent sources of pollution, e.g., collector and river drains, illegal ballast water discharges. For such slick bands, the local surface velocity is directed along the band axis, and its module can be retrieved as a function of width. To determine the coefficient of this function, which depends on a concentration and an origin of surfactant substance, contact measurements of environmental conditions are required at any point of the band. Performing these measurements will make it possible to estimate the surface speed at a measuring point (as the sum of the flow in the upper layer and 3% from the wind speed), which in conjunction with the measurements of band width will allow to estimate the surfactant concentration in the entire band.

Combination of such an experiment with obtaining a satellite radar image of sea surface with high spatial resolution will allow a thin structure of surface velocity (both module and direction) to be retrieved along the band axis at large distances from the source of surfactant. To study the structure of submesoscale vortices (up to dozens of km) in the absence of wind fronts over sea surface at the time of satellite imaging, heterogeneity of wind field can usually be neglected. In this case, the velocity of the marine current can be retrieved by subtracting the wind component from the surface velocity. According to the literature, up to 90% of vortex structures observed in radar images, particularly, of inland seas, appear due to the “slick mechanism” [33]. The results obtained in this paper indicate that the contribution of wind to the slick band propagation should be taken into account. Despite the fact that slick band structures are often observed at relatively weak winds (3–6 m/s), the contribution of the wind component can be comparable to the current one. This factor may significantly influence on the spatial characteristics of the band propagation, which finally may lead to incorrect estimation of the vortex scale and structure.

Marine surface films, either biogenic or anthropogenic, have elasticity values which vary widely, i.e., typically from about 5 to 30 mN/m [3,34,35]. Film slicks with such elasticity values are distinctively seen in radar imagery at low-to-moderate wind conditions, since the radar contrast (damping ratio) that is the ratio between radar backscatter in the background clean water and in slick can achieve 10 dB or greater, depending on Bragg wavelengths [3,36,37]. Surfactant films, which are usually used in experiments with artificial slicks, are characterized by similar elasticity values [31].

4. Conclusions

In conclusion, we briefly summarize the main results of this paper:

1. A new experimental approach to the registration of the structure of near surface currents has been developed. The methodology is based on the use of artificial slick bands with pre-measured physical film characteristics for tracking marine surface currents. The developed methodology can be efficient for performing sub-satellite experiments, for example, using high-resolution satellite radar data in combination with quasi-synchronous meteorological measurements at any point of the artificial slick band.

2. The formation of a slick band has been studied in the experiment and empirical relations between the geometric characteristics of the band and the characteristics of the surface velocity have been obtained, including the band width and the concentration of surfactants in the band. It has been shown that the geometry of the band is determined not only by the structure of current, but also by the contribution of the near-surface wind component. With a constant source of surfactant,

the concentration of a substance in a band can be considered roughly constant. It makes it possible to relate the width of the band and the surface velocity by a simple relationship; the latter has been verified in experiment.

3. The conditions of applicability of the suggested experimental approach, with an aim of evaluating surface velocities and determining the structure of currents based on images of the sea surface, have been determined, namely: (a) the absence of spreading processes in the slick band, (b) constant surfactant concentration and knowledge of concentration values for slick bands of different nature, (c) knowledge of wind velocity, uniformity of the near-surface wind field in observed area, (d) near-surface wind speeds of 2–10 m/s, absence of sharp changing of wind direction during the experiment.

The originality of the approach is based on the use of quasi-stationary slick bands in conditions when the influence of spreading effects can be neglected. Empirical relations between the geometric characteristics of the band and the characteristics of surface velocity are obtained. The advantage of this approach is the possibility of obtaining information about the spatial structure of marine currents along the entire slick band based on meteorological measurements conducted at any point of the band. This approach can be applied to the verification of satellite data.

Further studies will aim at conducting complex sub-satellite experiments. This will make it possible to observe the dynamics of banded structures on significantly larger scales and to retrieve current rates far from the source of surfactant. It will also allow the validation of the proposed approach in other conditions, including various orientations of wind and current velocities as well as different ratio between their speeds and under conditions of spatially-inhomogeneous near-surface currents. The acquisition of data regarding concentrations and characteristic consumptions of slick bands, caused by sources of different nature, may make it possible to retrieve current structures using radar images of sea surface without contact measurements. The methodology for obtaining and using a database of typical surfactant concentrations in localized anthropogenic sources, for example, illegal ship discharges, collector and river drains, is an interesting task for future work.

Supplementary Materials: The following are available online at <http://www.mdpi.com/2072-4292/11/7/840/s1>, Video “Artificial slick band propagation”.

Author Contributions: I.A.K. carried out experiments, analyzed the results and wrote the paper, A.V.E., and N.A.B. processed the experimental data, O.V.S. and S.A.E. analyzed the results and wrote the paper, A.V.K. and A.A.M. participated in experiment.

Funding: This research was funded by the Russian Science Foundation (Project RSF 18-77-10066).

Acknowledgments: We would like to thank all anonymous reviewers for their constructive comments, which helped to improve the paper. We are also grateful to the staff of the English Language Department of the Volga State University of Water Transport and personally to Yu.R. Guro-Frolova for their help in paper translation.

Conflicts of Interest: The authors declare no conflict of interest.

References

1. Gade, M.; Byfield, V.; Ermakov, S.; Lavrova, O.; Mitnik, L. Slicks as indicators for marine processes. *Oceanography* **2013**, *26*, 138–149. [[CrossRef](#)]
2. Da Silva, J.C.B.; Ermakov, S.A.; Robinson, I.S.; Jeans, D.R.G.; Kijashko, S.V. Role of surface films in ERS SAR signatures of internal waves on the shelf 1. Short-period internal waves. *J. Geophys. Res.* **1998**, *103*, 8009–8031. [[CrossRef](#)]
3. Ermakov, S.A.; Panchenko, A.R.; Salashin, S.G. Film slicks on the sea surface and some mechanisms of their formation. *Dyn. Atmos. Oceans* **1992**, *16*, 279–304. [[CrossRef](#)]
4. Lavrova, O.Y.; Mityagina, M.I.; Kostianoy, A.G. *Satellite Methods for Detecting and Monitoring Marine Zones of Ecological Risk*; ISR RAS: Moscow, Russia, 2016; pp. 101–306.
5. Johannessen, J.A.; Shuchman, R.A.; Digranes, G.; Lyzenga, D.R.; Wackerman, C.; Johannessen, O.M.; Vachon, P.W. Coastal ocean fronts and eddies imaged with ERS 1 synthetic aperture radar. *J. Geophys. Res.* **1996**, *101*, 6651–6667. [[CrossRef](#)]

6. Ivanov, A.Y.; Ginzburg, A.I. Oceanic eddies in synthetic aperture radar images. *J. Earth Syst. Sci.* **2002**, *111*, 281–295. [[CrossRef](#)]
7. Lavrova, O.; Serebryany, A.; Bocharova, T.; Mityagina, M. Investigation of fine spatial structure of currents and submesoscale eddies based on satellite radar data and concurrent acoustic measurements. In *Remote Sensing of the Ocean, Sea Ice, Coastal Waters, and Large Water Regions*; International Society for Optics and Photonics: Edinburgh, UK, 2012; Volume 8532.
8. Lavrova, O.Y.; Mityagina, M.I.; Sabinin, K.D.; Serebryany, A.N. Study of hydrodynamic processes in the shelf zone based on satellite data and subsatellite measurements. *Sovrem. Problemy Distantionnogo Zondirovaniya Zemli iz Kosmosa* **2015**, *12*, 98–129.
9. Lavrova, O.Y.; Sabinin, K.D. Fine spatial structure of flows on satellite radar image of the Baltic Sea. *Doklady Earth Sci.* **2016**, *467*, 427–431. [[CrossRef](#)]
10. Espedal, H.A.; Johannessen, O.M.; Johannessen, J.A.; Dano, E.; Lyzenga, D.R.; Knulst, J.C. COASTWATCH'95: ERS 1/2 SAR detection of natural film on the ocean surface. *J. Geophys. Res.* **1998**, *103*, 24969–24982. [[CrossRef](#)]
11. Ermakov, S.; Kapustin, I.; Sergievskaya, I. Remote sensing and in situ observations of marine slicks associated with inhomogeneous coastal currents. In *Remote Sensing of the Ocean, Sea Ice, Coastal Waters, and Large Water Regions*; International Society for Optics and Photonics: Prague, Czech Republic, 2011; Volume 8175.
12. Ochadlick, J.A.R.; Cho, P.; Evans-Morgis, J. Synthetic aperture radar observations of currents colocated with slicks. *J. Geophys. Res.* **1992**, *97*, 5325–5330. [[CrossRef](#)]
13. Zhurbas, B.M. The principle mechanisms of oil distribution in the sea. In *Mechanics of Fluid and Gas*; VINITI: Moscow, Russia, 1978; pp. 144–159.
14. Fingas, M. *Oil Spill Science and Technology*, 2nd ed.; Elsevier, Gulf Professional Publishing: Edmonton, AB, Canada, 2016; pp. 419–453.
15. Wu, J. Sea-surface drift currents induced by wind and waves. *J. Geophys. Res.* **1983**, *13*, 1441–1451. [[CrossRef](#)]
16. Malinovsky, V.V.; Dulov, V.A.; Korinenko, A.E.; Bol'shakov, A.N.; Smolov, V.E. Field investigations of the drift of artificial thin films on the sea surface. *Izvestiya Atmos. Ocean. Phys.* **2007**, *43*, 103–111. [[CrossRef](#)]
17. Ermakov, S.; Kapustin, I.; Molkov, A.; Leshev, G.; Danilicheva, O.; Sergievskaya, I. Remote sensing of evolution of oil spills on the water surface. In *Remote Sensing of the Ocean, Sea Ice, Coastal Waters, and Large Water Regions*; International Society for Optics and Photonics: Berlin, Germany, 2018; Volume 10784.
18. Halverson, M.; Pawlowicz, R.; Chavanne, C. Dependence of 25-MHz HF Radar Working Range on Near-Surface Conductivity, Sea State, and Tides. *J. Atmos. Ocean. Technol.* **2017**, *34*, 447–462. [[CrossRef](#)]
19. Mouche, A.A.; Collard, F.; Chapron, B.; Dagestad, K.F.; Guitton, G.; Johannessen, J.A.; Kerbaol, V.; Hansen, M.W. On the Use of Doppler Shift for Sea Surface Wind Retrieval From SAR. *IEEE Trans. Geosci. Remote Sens.* **2012**, *50*, 2901–2909. [[CrossRef](#)]
20. Ermakov, S.A.; Kapustin, I.A.; Sergievskaya, I.A. On peculiarities of scattering of microwave radar signals by breaking gravity-capillary waves. *Radiophys. Quantum Electron.* **2012**, *55*, 239–250. [[CrossRef](#)]
21. Ermakov, S.A.; Kapustin, I.A.; Sergievskaya, I.A. Tank Study of Radar Backscattering from Strongly Nonlinear Water Waves. *Bull. Russ. Acad. Sci. Phys.* **2010**, *74*, 1695–1698. [[CrossRef](#)]
22. Gade, M.; Alpers, W.; Ermakov, S.A.; Huehnerfuss, H.; Lange, P. Wind-wave tank measurements of bound and freely propagating short gravity-capillary waves. *J. Geophys. Res.* **1998**, *103*, 21697–21709. [[CrossRef](#)]
23. Plant, W.J. A model for microwave Doppler sea return at high incidence angles: Bragg scattering from bound, tilted waves. *J. Geophys. Res.* **1997**, *102*, 21131–21146. [[CrossRef](#)]
24. Ermoshkin, A.V.; Kapustin, I.A. Investigation of surfactant spreading over the surface of internal fresh-water reservoir using marine navigation radar. *Sovrem. Probl. Distantionnogo Zondirovaniya Zemli iz Kosmosa* **2015**, *12*, 72–79.
25. Ermakov, S.A.; Lavrova, O.Y.; Kapustin, I.A.; Makarov, E.V.; Sergievskaya, I.A. Investigation of geometry of film slicks on the sea surface from satellite radar observations. *Sovrem. Probl. Distantionnogo Zondirovaniya Zemli iz Kosmosa* **2016**, *13*, 97–105. [[CrossRef](#)]
26. Ermakov, S.A.; Ermoshkin, A.V.; Kapustin, I.A. On the effect of film slick compression. *Sovrem. Probl. Distantionnogo Zondirovaniya Zemli iz Kosmosa* **2017**, *14*, 288–294. [[CrossRef](#)]
27. Ermakov, S.A.; Lavrova, O.Y.; Kapustin, I.A.; Ermoshkin, A.V.; Molkov, A.A.; Danilicheva, O.A. On the “comb” structure of the edges of slicks on the sea surface. *Sovrem. Probl. Distantionnogo Zondirovaniya Zemli iz Kosmosa* **2018**, *15*, 208–217. [[CrossRef](#)]

28. Ermakov, S.A.; Sergievskaya, I.A.; da Silva, J.C.; Kapustin, I.A.; Shomina, O.V.; Kupaev, A.V.; Molkov, A.A. Remote Sensing of Organic Films on the Water Surface Using Dual Co-Polarized Ship-Based X-/C-/S-Band Radar and TerraSAR-X. *Remote Sens.* **2018**, *10*, 1097. [[CrossRef](#)]
29. Sergievskaya, I.A.; Ermakov, S.A.; Ermoshkin, A.V.; Kapustin, I.A.; Molkov, A.A.; Danilicheva, O.A.; Shomina, O.V. Modulation of Dual-Polarized X-Band Radar Backscatter Due to Long Wind Waves. *Remote Sens.* **2019**, *11*, 423. [[CrossRef](#)]
30. Fay, J.A. The spread of oil slicks on a calm sea. In *Oil on the Sea*; Hoult, D.P., Ed.; Plenum Press: New York, NY, USA, 1969; pp. 53–63.
31. Ermakov, S.A.; Kijashko, S.V. Laboratory study of the damping of parametric ripples due to surfactant films. In *Marine Surface Films*; Gade, M., Huehnerfuss, H., Korenovski, G., Eds.; Springer: Berlin/Heidelberg, Germany, 2006; pp. 113–128.
32. Elfouhaily, T.; Chapron, B.; Katsaros, K.; Vandemark, D. A unified directional spectrum for long and short wind-driven waves. *J. Geophys. Res.* **1997**, *102*, 15781–15796. [[CrossRef](#)]
33. Mityagina, M.I.; Lavrova, O.Y.; Karimova, S.S. Multi-sensor survey of seasonal variability in coastal eddy and internal wave signatures in the north-eastern Black Sea. *Int. J. Remote Sens.* **2010**, *31*, 4779–4790. [[CrossRef](#)]
34. Barger, W.R.; Daniel, W.H.; Garrett, W. Surface chemical properties of banded slicks. *Deep Sea Res.* **1974**, *21*, 83–89. [[CrossRef](#)]
35. Frew, N.M.; Nelson, R.K. Scaling of marine microlayer film surface-pressure isotherms using chemical attributes. *J. Geophys. Res.* **1992**, *97*, 5291–5300. [[CrossRef](#)]
36. Gade, M.; Alpers, W.; Huehnerfuss, H.; Masuko, H.; Kobayashi, T. Imaging of biogenic and anthropogenic ocean surface films by the multifrequency/multipolarization SIR_C/X-SAR. *J. Geophys. Res.* **1998**, *103*, 18851–18866. [[CrossRef](#)]
37. Alpers, W.; Huehnerfuss, H. The damping of ocean waves by surface films: A new look at an old problem. *J. Geophys. Res.* **1989**, *94*, 6251–6266. [[CrossRef](#)]



© 2019 by the authors. Licensee MDPI, Basel, Switzerland. This article is an open access article distributed under the terms and conditions of the Creative Commons Attribution (CC BY) license (<http://creativecommons.org/licenses/by/4.0/>).